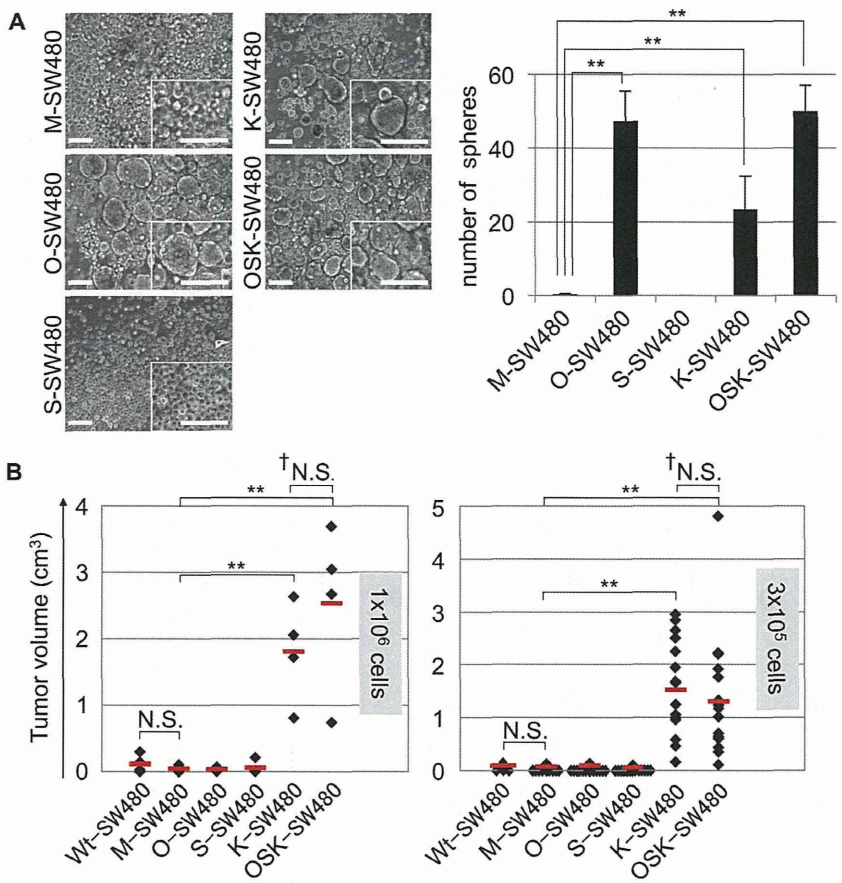


**Figure 2. The sphere formation ability *in vitro* and tumorigenicity *in vivo*.** (A) The spheroid formation assay. A total of $1\times10^4$ cells were plated on low attachment dishes on day 10 and cultured with serum-free medium for 10 days. In the O-, K- and OSK-SW480 cultures, the number of spheroids was significantly increased compared to that of the M-SW480 cells. The error bars indicate the SD (n = 3). Scale bars: 100 μm. (B) The tumorigenicity of the cells after implantation in the subcutaneous regions of immunodeficient nude mice. A total of $1\times10^6$ cells (left panel) or $3\times10^5$ cells (right panel) were subcutaneously injected into both flanks of immunodeficient nude mice on day 10. The volume of the tumors derived from the K- and OSK-SW480 cells were obviously higher than those of the Wt-, M-, O- and S-SW480 cells for both numbers of injected cells. The red bars indicate the median tumor volume. **P<0.01, N.S.: not significant, Dunnett's test (except of †: U-test).
doi:10.1371/journal.pone.0101735.g002

and 5.0%, respectively) compared to the M-SW480 culture (2.6%) (Fig. 3A, right panel). Notably, unique cells, which were unlabeled by Hoechst33342 even with the presence of 50 μM of VM, were obvious in the OSK-SW480 cultures. We termed these cells as "V50-cells" (Fig. 3A, left panel). Treatment with 250 μM of VM resulted in the disappearance of the cells within the gate, indicating that the V50-cells were sensitive to 250 μM of VM (Fig. 3B, left panel). Taken together, these data indicated that we

**Table 1.** Summary of tumor formation derived from transduced SW480 cells.

| | Tumor formation | |
|---|---|---|
| | Injected cell number | |
| **Cell name** | **$1\times10^6$** | **$3\times10^5$** |
| Wt-SW480 | 75% (3/4) | 25% (1/4) |
| M-SW480 | 75% (3/4) | 25% (3/12) |
| O-SW480 | 75% (3/4) | 25% (4/16) |
| S-SW480 | 75% (3/4) | 25% (4/16) |
| K-SW480 | 100% (4/4) | 100% (16/16) |
| OSK-SW480 | 100% (4/4) | 100% (*17/16) |

*In one case, we observed 2 tumors in one injected region.
doi:10.1371/journal.pone.0101735.t001

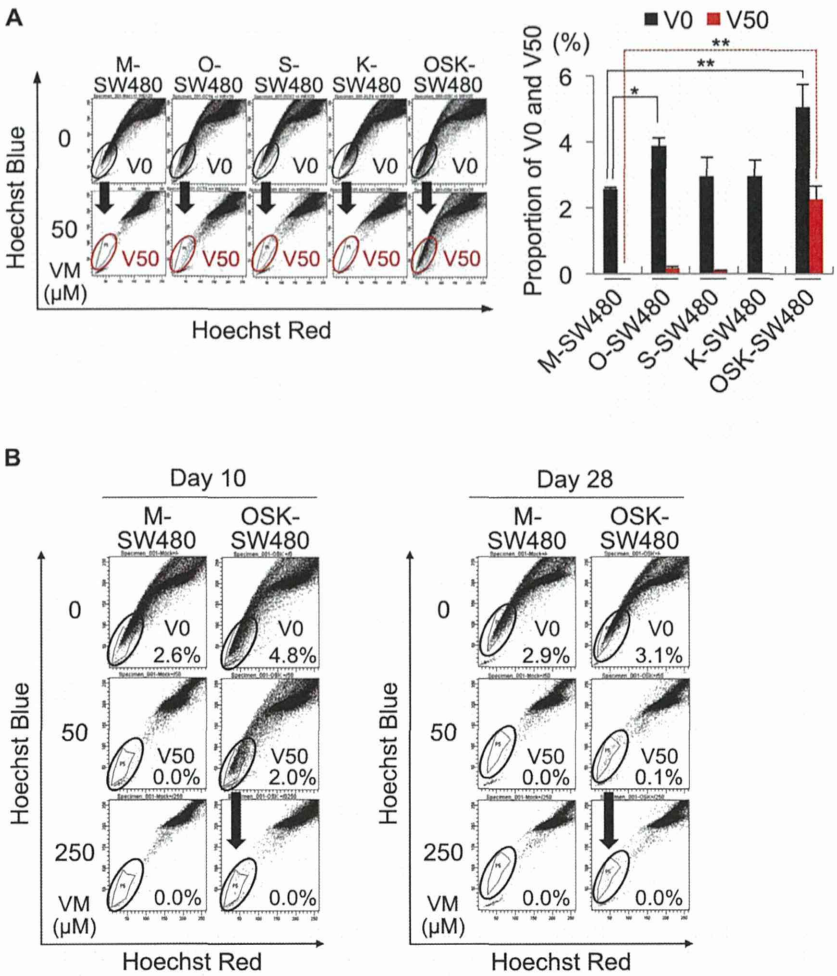


**Figure 3. Efflux activity for Hoechst33342.** (A) The OSK-SW480 cells included a population of cells unlabeled by 5 μg/ml of Hoechst33342 with the co-administration of 50 μM of verapamil (VM). We designated the cells unlabeled by Hoechst33342 without VM and with 50 μM of VM as V0-cells and V50-cells, respectively. The left panel shows representative dot plots of labeled and unlabeled cells at day 10 after transduction. The right panel shows the results of three independent experiments. The V0 subpopulation was increased in the O- and OSK-SW480 cells. The V50-cells were obviously seen in the OSK-SW480 cultures. The error bars indicate the SD (n = 3). *P<0.05, **P<0.01, Dunnett's test. (B) Dye efflux activity at day 10 (left panel) and day 28 (right panel) after transduction. The V50-cells disappeared under the treatment with the co-administration of 250 μM of VM even in the OSK-SW480 cells. The proportion of the OSK-V50 cells decreased with time.
doi:10.1371/journal.pone.0101735.g003

obtained a new collectable cell population: V50-cells with a highly potent dye-efflux activity induced in the OSK-SW480 cultures.

## Confirmation with another colon cancer cell line

To confirm the current results, we examined another colon cancer cell line, DLD-1, in some experiments, including evaluations of the cell growth rate *in vitro*, tumorigenicity *in vivo* and the Hoechst33342 effluxing properties (Fig. S4). In the DLD-1 cells, the growth rate of the OSK-DLD-1 cells was lower than that of the Wt- (parental) and Mock-DLD-1 cells ($p<0.01$, $n=3$) (Fig. S4A). The tumorigenicity of $1\times10^5$ cells was higher in OSK-DLD-1 cells compared to Wt- and Mock-DLD-1 cells (Fig. S4B, Table S2). V50-cells were also seen in the OSK-DLD-1, but not in the Mock-DLD-1, cultures (Fig. S4C).

## Collecting the iCSCs from OSK-SW480

To examine whether the CSC properties induced in OSK-SW480 cultures were attributable to V50-cells, we sorted and analyzed the V50-cells and non-V50-cells in the presence of 50 μM of VM in OSK-SW480 cells, and V0-cells and non-V0-cells in the absence of VM and non-V50-cells in the presence of 50 μM of VM in the M-SW480 cultures. These cells were termed OSK-V50, OSK-nonV50, M-V0, M-nonV0 and M-nonV50, respectively.

After sorting by a fluorescence-activated cell sorter (FACS) on day 10, all the lines were subsequently cultured for 10 days in DMEM containing 10% FBS. The OSK-V50 cells exhibited morphology similar to that distinctively observed in the OSK-SW480 cells on day 10 (Fig. 4A, Fig. S1D). In contrast, the OSK-nonV50 cells exhibited morphology similar to that of the M-V0, M-nonV0 and M-nonV50 cells (Fig. 4A). The cell growth rate of the OSK-V50 cells was significantly lower than that of the other lines ($p<0.01$, $n=3$) (Fig. 4B), resulting in decreased proportion (~0.1%) of the V-50 cells at 28 days after transduction under the current culture condition (Fig. 3B, right panel).

The tumorigenicity of the OSK-V50 cells in the immunodeficient mice was obviously higher in terms of the size and incidence

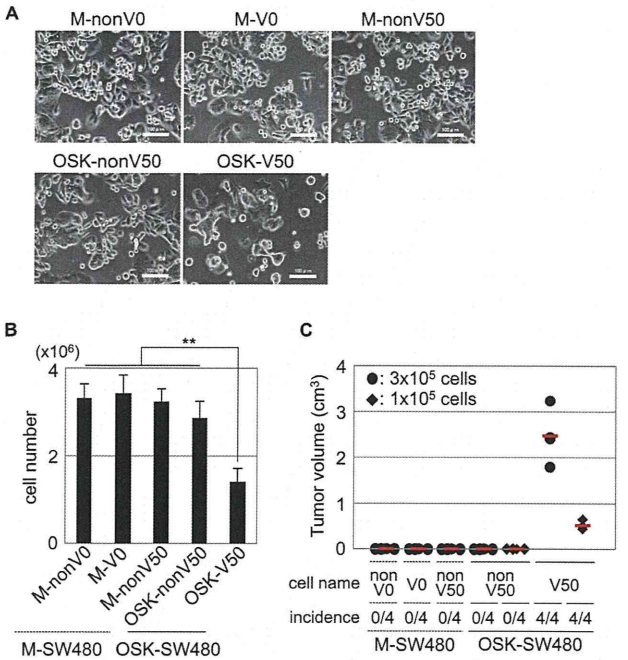


**Figure 4. Characterization of the V50-cells in OSK-SW480 cells after FACS.** The V50-cells in the OSK-SW480 (OSK-V50) cells were sorted by FACS. Non-V0-, V0- and non-V50-cells in the M-SW480 cells (M-nonV0, M-V0 and M-nonV50, respectively) and non-V50-cells in the OSK-SW480 cells (OSK-nonV50) were also sorted and used as controls. These cells were all subsequently cultured. (A) The morphologies of the cells cultured for 10 days after sorting. The morphology of the OSK-V50 cells was similar to that distinctively observed in OSK-SW480 cells (Fig. S1D, lined circle). In contrast, the morphology of OSK-nonV50 cells was similar to that of M-V0, M-nonV0 and M-nonV50 cells. Scale bars: 100 μm. (B) The cell proliferation *in vitro*. A total of $3\times10^5$ cells cultured for 14 to 18 days after sorting were seeded and counted 96 hr later. The number of cells was significantly lower in the OSK-V50 cells than that in all the other lines. The error bars indicate the SD (n = 3). **P<0.01, Scheff's test. (C) Tumorigenicity of the cells in immunodeficient mice. A total of $3\times10^5$ or $1\times10^5$ cells were subcutaneously injected into immunodeficient nude mice on day 18 after sorting. The tumor volume and incidence were measured eight weeks after injection. Only the OSK-V50 cells generated obvious tumors for both the injected cell numbers, whereas no tumors were obtained from the M-nonV0, M-V0, M-nonV50 and OSK-nonV50 cells. The incidence of tumor formation by OSK-V50 cells was 4/4 for both injected cell numbers. The red bars indicate the median tumor volume.
doi:10.1371/journal.pone.0101735.g004

of tumors than that of the other cell lines, including OSK-nonV50 cells (Fig. 4C).

Taken together, these data indicate that the OSK-V50 cells exhibited CSC properties, but that the OSK-nonV50 cells did not, indicating that the CSC properties induced in OSK-SW480 cells were attributable to the V50-cell population.

## Colonic lineage differentiation of OSK-V50 cells *in vitro*

OSK-V50 cells as well as M-V0 cells were positive for CDX2, a master regulator of intestinal epithelial differentiation [25], and CK20, a colonic differentiation marker [26], by immunostaining (Fig. 5A). Thus OSK-V50 cells maintained colonic lineage phenotype and differentiation ability *in vitro* (Fig. 5A).

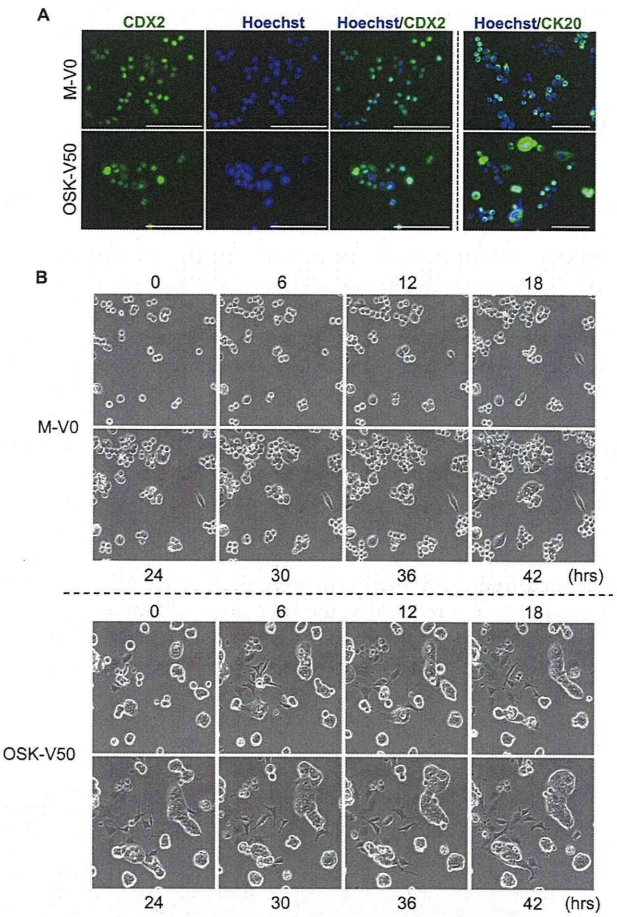


**Figure 5. Colonic lineage specificity and potency to produce phenotypical diversity in OSK-V50 cells.** (A) Immunocytochemistry for CDX2 and CK20 protein. OSK-V50 cells were positive for CDX2 and CK20, as well as M-V0 cells. The cells were counterstained with Hoechst33342. Scale bars: 100 μm. (B) The phenotypical diversity in morphology and mobility of derivatives of OSK-V50 cells. Photographs are time-lapse images of M-V0 and OSK-V50 cells. The sorted cells were subsequently cultured for five days and then observed every six hours for 42 hr. Time-lapse imaging revealed that there was a higher diversity in both the morphology and mobility in OSK-V50 cells (lower panel) compared to M-V0 cells (upper panel). Original magnification, ×20. Movies of M-V0 and OSK-V50 cells are shown in Video S1 and Video S2, respectively.
doi:10.1371/journal.pone.0101735.g005

## Phenotypical diversity in derivatives of OSK-V50

Generating heterogeneity in cancer tissues is one of the notable CSC properties [1–3]. To examine this property in our isolated cells, we subsequently analyzed 23 days after sorting (Fig. S5). The OSK-V50 cells, in contrast to all the other cells, could produce V50-cells and as well as diverse different subsets of cells in terms of the degree of Hoechst-effluxing function (Fig. S5).

We next performed *in vitro* time-lapse imaging of M-V0 and OSK-V50 cells for 42 hr (Fig. 5B, Methods S1). The M-V0 cells consisted of small round- and spindle-shaped cells, and formed colonies consisting of cells with clear edges. The OSK-V50 cells consisted of cells with various morphologies, such as polygonal-, round-, cuboidal-, spindle- and flat-shaped cells, which altered their morphologies with time, and formed flat-mounted colonies consisting of cells with unclear edges. Furthermore, the OSK-V50 cells exhibited higher cell mobility than the M-V0 cells (Fig. 5B,

Videos S1 and S2). These results suggest that OSK-V50 cells can produce a higher diversity in terms of morphology and mobility compared to M-V0 cells.

## Colonic lineage differentiation of OSK-V50 cells *in vivo*

We next histologically assessed the tumors derived from the M-SW480 and OSK-V50 cells in immunodeficient mice (Fig. 6). The tumors derived from the M-SW480 cells predominantly consisted of the homogeneous and monotonous expansion of uniform dysplastic cells. In contrast, in the tumors derived from OSK-V50 cells, we observed cell diversity and glandular structures, which are often present in human colorectal cancer tissues (Fig. 6A).

In addition, we performed an immunohistochemical analysis (Fig. 6B). Typical human colon cancer tissues are positive for CK20 and CDX2, and negative for CK7 [27,28]. The tumors derived from the M-SW480 cells were negative for CK20 and CK7. In contrast, the tumors derived from OSK-V50 cells were partially positive for CK20 and negative for CK7, which was consistent staining pattern with actual human colon cancer tissues [29,30]. Together OSK-V50 cells showed colonic lineage phenotype and differentiation ability *in vivo*. Furthermore, the tumors generated from M-SW480 cells were positive for CDX2, whose expression level is reduced in the later stages of human colorectal cancer and invasive cancer indicated by an immunohistochemical study [31]. The tumors derived from OSK-V50 cells were also positive for CDX2, whereas these tumors contained more CDX2-negative cells than the tumors derived from M-SW480.

These data demonstrated that the tumors of OSK-V50 cells represented a similar in histological and immunohistochemical characteristics to actual human colon cancer tissues.

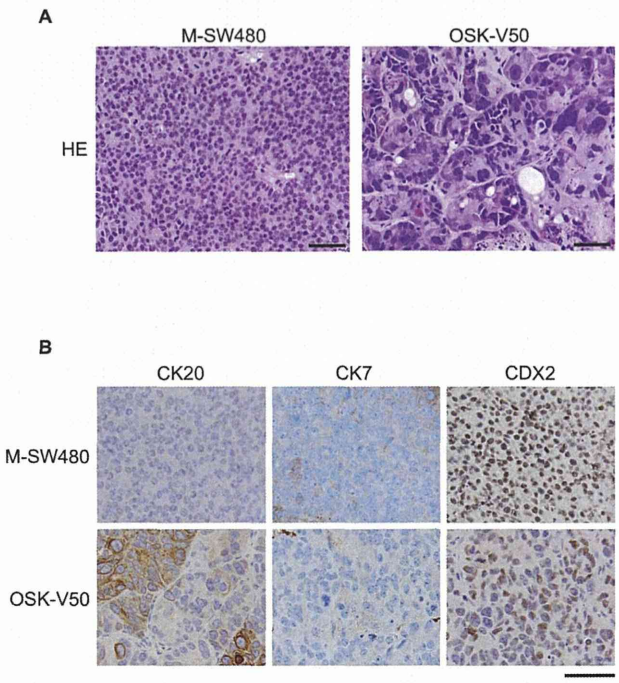


**Figure 6. The histology of the xenografts derived from M-SW480 and OSK-V50 cells.** (A) Hematoxylin and eosin staining (HE). The tumors derived from M-SW480 cells predominantly consisted of homogeneous cells. On the other hand, the tumors derived from OSK-V50 cells showed glandular structures. (B) Immunohistochemical analysis. The tumors derived from M-SW480 cells were negative for CK20 and CK7. The tumors derived from OSK-V50 cells were partially positive for CK20 and negative for CK7. Tumors derived from both M-SW480 and OSK-V50 cells were positive for CDX2, but CDX2-negative cells were obviously seen in the tumors of OSK-V50 cells. Scale bars: 50 μm.
doi:10.1371/journal.pone.0101735.g006

## Self-renewal capacity of the OSK-V50 cells *in vivo*

To examine whether the OSK-V50 cells could self-renew *in vivo*, we next performed serial transplantation experiments (n = 3). A schematic representation of the serial transplantation experiments is shown in Figure 7A. In this experiments, a total of $3\times10^6$ cultured OSK-V50 cells (first cultured cells) were subcutaneously injected into nude mice. The tumors derived from these first cultured cells were dissociated, and the dissociated cells were subsequently cultured (second culture) *in vitro*. The tumors and the dissociated cells were analyzed. We repeated the procedure three times until the fourth culture of cells. From the OSK-V50 cells, we could serially obtain tumors large enough for the following procedures. Whereas in the case of M-nonV50 cells which we used as control cells in this experiments, the transplantation of M-nonV50 cells at the same number as that used for the OSK-V50 cells led to the formation of only a small nodule. Therefore, we injected a total of $8–10\times10^6$ cells from the first cultured M-nonV50 cells, and performed the serial transplantation experiments only once until the second culture of M-nonV50 cells.

The first, second, third and fourth serially cultured OSK-V50 cells showed the same morphological characteristics, which were similar to those shown in Figures 4A and 5B (Fig. 7B). The number of OSK-V50 cells 72 hr after seeding $2\times10^5$ cells was significantly lower than that of M-nonV50 cells in the second culture (Fig. 7C) ($p<0.01$, n = 3). In the dye efflux activity analysis, the proportion of V50 cells was 1–1.6% in the second, third and fourth cultures of cells in case of the OSK-V50 cells, whereas no V50 cells were observed in the second culture of the M-nonV50 cells (Figs. 7D and S6). In addition, the first, second and third tumors serially derived from the OSK-V50 cells exhibited the same histological and immunohistochemical findings, which were similar to actual human colon cancer tissues, as shown in Figure 6 (Figs. 7E and S7). In contrast, the tumors derived from M-nonV50 cells showed the same features as those of the M-SW480 cells shown in Figure 6, not the same as the findings seen for OSK-V50 cells. These data indicated that the OSK-V50 cells showed self-renewal capacity in the serial *in vivo* transplantation studies.

## Characterization of the re-sorted V50 cells from tumors

We next collected V50 and non-V50 cells from the third cultured OSK-V50 cells by FACS sorting based on the dye-effluxing ability of the cells, and analyzed the cells (n = 3) (Fig. S8A). The number of the re-sorted V50 cells 96 hr after seeding $3\times10^5$ cells was significantly lower than that of the re-sorted non-V50 cells ($p<0.01$, n = 3) (Fig. S8B). The re-sorted V50 cells exhibited the same morphological features as the OSK-V50 cells, as shown in Figures 4A and 5B, showing a higher diversity in their morphologies with time (Fig. S8C). A total of $3\times10^6$ cells of the re-sorted V50 cells cultured for five to six days were subcutaneously injected into nude mice. The tumors derived from the re-sorted V50 cells showed the same pathological findings as the first, second and third tumors (Fig. S8D). The proportion of V50 cells in the cultured cells from tumors derived from the re-sorted V50 cells was 1.3–2.7% (Fig. S8E). These data support that the re-sorted V50 cells can also self-renew *in vivo*.

In summary, we generated the cells with CSC properties: iCSCs, by introducing *OCT3/4*, *SOX2* and *KLF4* in the SW480 colon cancer cell line, and were able to isolate an iCSCs-enriched

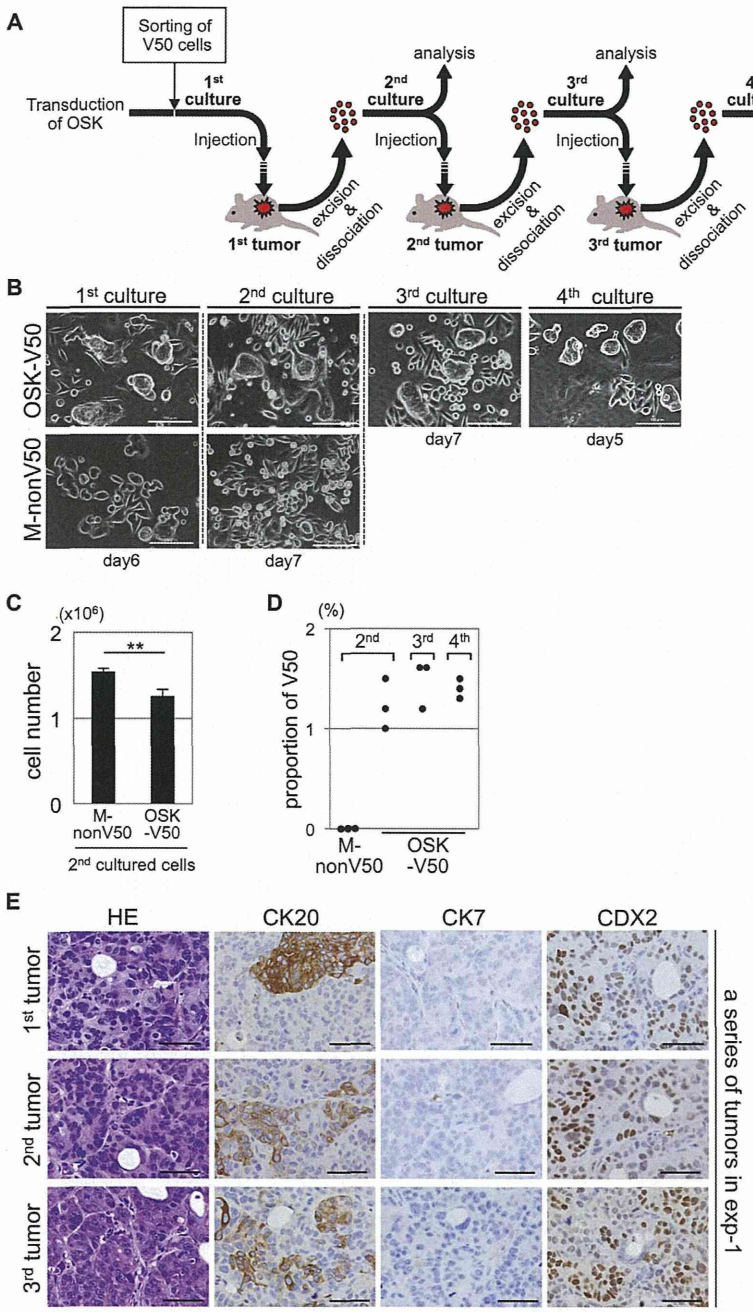


**Figure 7. The self-renewal capacity of the OSK-V50 cells *in vivo*.** (A) A schematic representation of serial transplantation experiments. (B) The morphological features of a series of cultured cells in the serial transplantation experiments. The day shown under the panel indicates the culture period after sorting for the first cultured cells and after dissociation from tumors for the second, third and fourth cultured cells. In the case of OSK-V50 cells, the morphological features in each culture were the same over three passages *in vivo*, and the features were similar to those shown in Figures 4A and 5B. Scale bars: 100 μm. (C) The cell proliferation of the second cultured cells *in vitro*. A total of $2\times10^5$ cells cultured for four to six days after dissociation were seeded and counted 72 hr later. In the second cultured cells, the number of OSK-V50 cells was significantly lower than that of M-nonV50 cells (n = 3). **P<0.01, t-test. (D) The proportion of V50 cells in the second, third and fourth cultured cells. The panel shows the proportion of V50 cells in each culture from three independent experiments. The V50 cells were maintained over three passages *in vivo*, whereas V50 cells were not observed in the second M-nonV50 cultured cells. The representative dot plots obtained by FCM are shown in Figure S6. (E) The pathological findings of xenograft tumors derived from OSK-V50 cells. The panel shows the histological findings of a series of tumors obtained from serial transplantation experiments. The results of the other series of tumors are shown in Figure S7. The OSK-V50 cells serially showed the same pathological findings as those described in Figures 6A and 6B; there was cell diversity and glandular structures observed by HE staining, and CK20- and CDX2-positive, and CK7-negative findings for the immunostaining. exp: experiment. Scale bars: 50 μm.
doi:10.1371/journal.pone.0101735.g007

cell population by using Hoechst33342 staining and VM treatment. The tumors derived from the iCSCs exhibited a more similar phenotype to *bona fide* colon cancer than did those from the parental SW480 cell line.

## Discussion

In this study, we found that a subset of colon cancer cells sufficiently acquired the colon CSC properties by introduction of OSK. It was previously reported that these transcription factors can convert somatic cells into iPSCs [7,8] and neural stem cells depending on their culture conditions [9]. Therefore, in the current study, we considered that OSK directly induced a cell-fate conversion to a CSC state in a subset of SW480 cells under their primary culture conditions, not *via* an iPSCs state.

Our data showed that forced expression of OSK could directly generate colon CSCs from colon cancer cells. On the other hand, recent studies reported that "CSCs" could be generated from iPSCs in both mouse [4] and human studies [5]. In a mouse study, CSCs giving rise to "adenocarcinoma" could be generated from iPSCs derived from normal mouse embryonic fibroblasts. In a human study, iPSCs-derived CSCs, whose origin was human mammary epithelial cells, could form "multilineage tumors". However, the iPSCs-derived CSCs in both cases were originally generated from "non-cancer cells". It is generally considered that cancer initiation involves genetic changes [32]. The tumors from the iPSCs-derived CSCs in both reports were less likely to have the pathogenic genetic changes associated with "cancer", therefore, it is still unclear whether the iPSCs-derived CSCs represent the CSC properties present in actual cancer cells which carry oncogenic genetic alterations. It should be noted that in this study, we succeeded in generating iCSCs from SW480 colon cancer cells, which have a pathogenic genome of "colon cancer".

In the current study, we were able to collect the cells with induced CSC properties based on their difference in the dye-efflux activity. We originally focused on the differences in the degree of efflux activity, and succeeded in establishing a new method to distinguish V50-cells from V0-cells in the OSK-SW480 cells by changing the concentration of VM. By using this method, we clarified that the forced expression of OSK induced not only an increase in the frequency of V0-cells existing in the SW480 cultures, but also the emergence of V50-cells that gained more enhanced effluxing activity.

The efflux pump activity is an important property in CSCs [33], because the efflux pump eliminates metabolic products and toxic compounds. Therefore, V50-cells are considered to be better able to preserve their survival even in a hostile environment, such as following treatment with chemotherapy or metastatic regions, in comparison to V0-cells that enriched primary CSCs [23,34]. CSCs are not uniform [2,35], thus it is important to consider not only the frequency of CSCs, but also the differences in the degree of their stemness.

The present results indicated that the OSK-V50 cells have colonic differentiation potency *in vitro* and *in vivo*. In the immunohistological study, the tumors derived from OSK-V50 cells mimicked *bona fide* colon cancer tissue and keep their lineage as colon cancer [27,28,36]. In contrast, the tumors of M-SW480 cells did not. We confirmed that these phenotypes of our iCSCs were reproducible in serial transplantation experiments using xenograft models. In addition, CK20 is well known as a marker of differentiation in colorectal cancer [26], therefore, the expression of CK20 in the xenografts of OSK-V50 cells suggests that OSK induced the ability of the OSK-V50 cells to differentiate, leading to higher cell diversity *in vivo*. These findings were consistent with the principle of a hierarchy as advocated by the CSC concept. In terms of the clinical applications of these cells, such as the development of anti-colon CSC drugs, it is critical to develop tumors that recapitulate *bona fide* colon cancers. The previous reports did not focus on the histology of tumors derived from iCSCs in detail, such as the structure, phenotypic diversity (based on the differentiation capacity of the iCSCs) and the lineage of the original tissues [4,5]. There exist "cancers of unknown origin", but not "cancers of no origin". Therefore, it is a significant point that the current method can allow for tumors similar to actual human colon cancer to be formed even in the subcutaneous region in mice.

In the current study, we could induce CSC properties in colon cancer cells by using an artificial system involving the forced expression of *OCT3/4*, *SOX2* and *KLF4*. Although these factors were individually reported to be correlated with the malignant behavior and poor prognosis in various cancers [37–42], it is unclear whether there are any cells that spontaneously overexpress *OCT3/4*, *SOX2* and *KLF4* in colon cancer tissues. Nevertheless, the important finding of this study was that the current colon iCSCs can form tumors similar to actual colon cancer, while the parental cell line could not. This finding implied that some kind of unknown OSK-downstream molecules might play a key role in our iCSCs, resulting in recapitulation of colon cancer tissues. Furthermore, if we identify the key molecules that are required for the development of actual colon CSCs, our iCSCs will help to establish CSC-targeting therapy by overcoming the sampling limitation of CSCs in clinical specimens. Therefore, a global analysis of the transcriptome, as well as carrying out proteomic and epigenomic studies could be useful to find such key molecules in future studies.

It could be a point of interest that only a small subset of transduced cells became iCSCs, and understanding the reason for this might help to better understand the generation of iCSCs. Although we did not evaluate the exact percentage of cells that expressed exogenous OCT3/4, SOX2 and KLF4 in the current study, there seemed to be a discrepancy between the percentage of OSK-V50 cells (~2%) and the retroviral transduction efficiency (~35% or more) of OSK inferred from Figure S1B, in which around half of the cells infected with the retrovirus mixture carrying one of three factors expressed both eGFP and DsRed. Therefore, the efficiency of the generation of the iCSCs might not simply reflect the transduction efficiency of OSK. It is still to be elucidated whether there are any mechanisms associated with suppressing the process of iCSC generation, like those seen for iPSC generation [43].

In addition, although we demonstrated that our iCSCs maintained their colon CSC nature *in vivo*, it is also still unclear whether the continuous presence of the exogenous OSK factors is needed for the maintenance of this colon CSC nature. To address this issue, it will be necessary to use a transient expression system for OSK in future studies.

In summary, we were able to generate colon iCSCs from an established colon cancer cell line by forced expression of OSK, and collect the iCSCs based on their difference in dye efflux activity. The iCSCs-derived cells and tissues were similar to actual human colon cancer tissue. By overcoming the quantitative limitations of primary human CSC samples and by dynamic observation of the CSC development, this method will enable us to elucidate the molecular mechanisms involved in the development and maintenance of CSCs, and will help to establish new therapies and diagnostic technology targeting CSCs.

## Supporting Information

**Figure S1** Transduction of *OCT3/4, SOX2, KLF4* or a mixture of the three factors (OSK) in SW480 cells. (A) A schematic representation of this study. (B) The transduction efficiency in SW480 cells. Cells were retrovirally transduced with a mixture of three factors; eGFP, DsRed and Mock (empty vector). Almost all cells expressed at least one the transduced genes. Around half of the cells expressed both eGFP and DsRed. Scale bar: 100 μm. (C) qRT-PCR of *OCT3/4*, *SOX2* and *KLF4* in transduced SW480 cells using primers common for both endogenous and exogenous transcripts. The mRNA expression levels were normalized to those of *GAPDH*. The relative expression levels compared to those to human iPSCs are shown. All the transduced genes were obviously expressed. The error bars indicate the SD (n = 3). † : not detected. (D) The morphology of the transduced SW480 cell lines. The transduction of each individual factor led to distinct morphological changes (arrow, dotted circle or arrow head). Simultaneous transduction of the three factors also led to specific morphologic features (lined circle). Parental cells (Wt-SW480) and M-SW480 cells predominantly consisted of spindle-shaped cells and small round-shaped cells. In the O-SW480 culture, globular clusters consisting of cells with unclear edges appeared. In the S-SW480 cultures, the number of round-shaped cells was increased. In K-SW480 cultures, colonies consisting of cells with slightly unclear edges appeared. In the OSK-SW480 cultures, flat-mounted colonies consisting of cells with unclear edges appeared, and similar morphologies were also seen as were noted in the other cells. Scale bars: 100 μm.
(PDF)

**Figure S2** The results of the flow cytometric (FCM) analysis of the CSC marker protein expression in transduced SW480 cells. The panel shows representative dot plots of the cells expressing CD133, CD44, CD26, ABCG2 and LGR5 in the transduced SW480 cells.
(PDF)

**Figure S3** Cell proliferation of transduced SW480 cells *in vitro*. The cell number of transduced SW480 cells was counted every four days from day 7 to day 27 after transduction. A growth curve of OSK-SW480 cells was lower than all the other cells at both the day 15 (upper panel) and the day 27 (lower panel). The error bars indicate the SD. (n = 3).
(PDF)

**Figure S4** Transduction of *OCT3/4, SOX2* and *KLF4* (OSK) into DLD-1 cells. A Mock (empty vector) or OSK was retrovirally transduced into DLD-1 cells (Mock-DLD-1, OSK-DLD-1, respectively). (A) The proliferation during a 72 hr period *in vitro*. A total of $3\times10^5$ cells were plated on six-well plates on day seven and were counted on day 10. The number of OSK-DLD-1 cells was significantly lower than that of the parental DLD-1 (Wt-DLD-1) and Mock-DLD-1 cells (n = 3). The error bars indicate the SD. $^{**}P<0.01$, Dunnett's test. (B) The tumorigenicity in immunodeficient mice. A total of $1\times10^5$ cells were subcutaneously injected into both flanks of immunodeficient nude mice on day 10. The tumor volume was measured eight weeks after injection. A summary of the tumor incidence is shown in Table S2. The volumes of tumors derived from the OSK-DLD-1 cells were significantly higher than those derived from Mock-DLD-1 cells. The red bars indicate the median tumor volume. $^{*}P<0.05$, N.S.: not significant, Dunnett's test. (C) Hoechst33342-efflux activity on day 10. The OSK-DLD-1 cells contained cells unlabeled by 5 μg/ml of Hoechst33342 with the co-administration of 50 μM of verapamil (VM). The V0-cells increased in the OSK-DLD-1 population. The V50-cells were obviously seen in OSK-DLD-1 culture. The V50-cells in OSK-DLD-1 were labeled by 5 μg/ml of Hoechst33342 with the co-administration of 250 μM of VM.
(PDF)

**Figure S5** The phenotypical diversity in efflux activity of derivatives of OSK-V50 cells. FCM analysis for the Hoechst33342-efflux activity of the sorted cells after 23 days in culture. The M-V0 cells produced V0-cells and non-V0-cells. The M-nonV50 cells, which consisted of M-V0 and M-nonV0 populations, produced V0-cells and non-V0-cells, but not V50-cells (upper panel). The OSK-nonV50 cells containing some OSK-V0 cells produced V0-, non-V0- and only a few V50-cells. In contrast, the OSK-V50 cells produced V0-, non-V0-, V50-, non-V50- and V250-cells, which are unlabeled by Hoechst33342 in the presence of 250 μM of VM (lower panel). VM: verapamil.
(PDF)

**Figure S6** The results of the dye efflux activity analysis of cultured cells dissociated from the tumors in serial transplantation experiments. The panel shows representative dot plots of the cells cultured for six to 12 days after dissociation. In the case of OSK-V50 cells, the V50 cells were serially observed in each of the sets of cultured cells. In contrast, V50 cells were not observed in the second cultured M-nonV50 cells. VM: verapamil.
(PDF)

**Figure S7** The pathological findings of the tumors in serial transplantation experiments. The upper and lower panels represent the pathological findings for each series of tumors in each serial transplantation experiment. The OSK-V50 cells serially showed the same pathological features as those described in Figures 6A and 6B; there was cell diversity and glandular structures noted in HE staining, and cells were CK20- and CDX2-positive and CK7-negative in the immunostaining studies. Scale bars: 50 μm.
(PDF)

**Figure S8** The characterization of the re-sorted V50 cells in serial transplantation experiments. (A) A schematic representation of the experiments. The V50 and nonV50 cells were re-sorted and collected from third cultured cells on day 9 after the dissociation of the second tumors by FACS sorting (n = 3). (B) The proliferation of re-sorted cells from the third cultured cells *in vitro*. A total of $3\times10^5$ cells cultured for 12 to 14 days after sorting were seeded and counted 96 hr later. The number of cells was significantly lower in the re-sorted V50 cells than in the re-sorted nonV50 cells (n = 3). $^{**}P<0.01$, t-test. (C) The morphologies of the re-sorted V50 and nonV50 cells. The day when each photograph was taken is indicated, and photographs were taken for each culture period after re-sorting. The re-sorted V50 cells exhibited morphological features similar to those of OSK-V50 cells, as shown in Figures 4A and 5B, resulting in an increase in cell diversity with time. Scale bars: 100 μm. (D) The pathological findings of tumors derived from re-sorted V50 cells in each independent experiment. The re-sorted V50 cells showed the same pathological features as those described in Figures 6A, 6B, 7E and S7; there was cell diversity and glandular structures observed by HE staining, and the immunostaining showed positive findings for CK20 and CDX2 and negative findings for CK7. Exp: experiment. Scale bars: 50 μm. (E) The results of the dye efflux activity analysis. The panel showed the data from three independent experiments subjected to a dye efflux activity analysis for the cells that were cultured for six to eight days after the dissociation of tumors derived from re-sorted V50 cells. VM: verapamil, Exp: experiment.
(PDF)

**Table S1** Primer sequences used in qRT-PCR.
(PDF)

**Table S2** Summary of tumor formation derived from transduced DLD-1 cells.
(PDF)

**Video S1** Time-lapse imaging of M-V0 cells.
(MOV)

**Video S2** Time-lapse imaging of OSK-V50 cells.
(MOV)

**Methods S1** (PDF)

## Acknowledgments

We thank Hisamori S, Hashimoto K, Semi K and Shimamoto R for valuable scientific discussion; members of Yamanaka and Yamada laboratory at CiRA for kind cooperation; Higuchi Y, Nishimoto N, Shibahara Y, Uemura F and Fujii C for administrative assistance; Kitamura K for pMXs retroviral vectors.

## Author Contributions

Conceived and designed the experiments: NO TA. Performed the experiments: NO. Analyzed the data: NO. Wrote the paper: NO TA. Histopathological analysis of the xenografts: YY. Interpretation and providing critical revision of the manuscripts for intellectual content: YY SN KK SH HO YS. Final approval of the version to be published: NO TA. Supervision of the project: TA.

## References

1. Reya T, Morrison SJ, Clarke MF, Weissman IL (2001) Stem cells, cancer, and cancer stem cells. Nature 414: 105–111.
2. Visvader JE, Lindeman GJ (2008) Cancer stem cells in solid tumours: accumulating evidence and unresolved questions. Nat Rev Cancer 8: 755–768.
3. Clevers H (2011) The cancer stem cell: premises, promises and challenges. Nature medicine 17: 313–319.
4. Chen L, Kasai T, Li Y, Sugii Y, Jin G, et al. (2012) A model of cancer stem cells derived from mouse induced pluripotent stem cells. PloS one 7: e33544.
5. Nishi M, Sakai Y, Akutsu H, Nagashima Y, Quinn G, et al. (2013) Induction of cells with cancer stem cell properties from nontumorigenic human mammary epithelial cells by defined reprogramming factors. Oncogene.
6. Zhang J, Espinoza LA, Kinders RJ, Lawrence SM, Pfister TD, et al. (2013) NANOG modulates stemness in human colorectal cancer. Oncogene 32: 4397–4405.
7. Takahashi K, Tanabe K, Ohnuki M, Narita M, Ichisaka T, et al. (2007) Induction of pluripotent stem cells from adult human fibroblasts by defined factors. Cell 131: 861–872.
8. Nakagawa M, Koyanagi M, Tanabe K, Takahashi K, Ichisaka T, et al. (2008) Generation of induced pluripotent stem cells without Myc from mouse and human fibroblasts. Nature biotechnology 26: 101–106.
9. Matsui T, Takano M, Yoshida K, Ono S, Fujisaki C, et al. (2012) Neural stem cells directly differentiated from partially reprogrammed fibroblasts rapidly acquire gliogenic competency. Stem Cells 30: 1109–1119.
10. Zhou S, Schuetz JD, Bunting KD, Colapietro AM, Sampath J, et al. (2001) The ABC transporter Bcrp1/ABCG2 is expressed in a wide variety of stem cells and is a molecular determinant of the side-population phenotype. Nature medicine 7: 1028–1034.
11. Kondo T, Setoguchi T, Taga T (2004) Persistence of a small subpopulation of cancer stem-like cells in the C6 glioma cell line. Proceedings of the National Academy of Sciences of the United States of America 101: 781–786.
12. Haraguchi N, Utsunomiya T, Inoue H, Tanaka F, Mimori K, et al. (2006) Characterization of a side population of cancer cells from human gastrointestinal system. Stem Cells 24: 506–513.
13. Todaro M, Francipane MG, Medema JP, Stassi G (2010) Colon cancer stem cells: promise of targeted therapy. Gastroenterology 138: 2151–2162.
14. Vaiopoulos AG, Kostakis ID, Koutsilieris M, Papavassiliou AG (2012) Colorectal cancer stem cells. Stem Cells 30: 363–371.
15. O'Brien CA, Pollett A, Gallinger S, Dick JE (2007) A human colon cancer cell capable of initiating tumour growth in immunodeficient mice. Nature 445: 106–110.
16. Ricci-Vitiani L, Lombardi DG, Pilozzi E, Biffoni M, Todaro M, et al. (2007) Identification and expansion of human colon-cancer-initiating cells. Nature 445: 111–115.
17. Dalerba P, Dylla SJ, Park IK, Liu R, Wang X, et al. (2007) Phenotypic characterization of human colorectal cancer stem cells. Proceedings of the National Academy of Sciences of the United States of America 104: 10158–10163.
18. Du L, Wang H, He L, Zhang J, Ni B, et al. (2008) CD44 is of Functional Importance for Colorectal Cancer Stem Cells. Clin Cancer Res 14: 6751–6760.
19. Pang R, Law WL, Chu ACY, Poon JT, Lam CSC, et al. (2010) A Subpopulation of CD26+ Cancer Stem Cells with Metastatic Capacity in Human Colorectal Cancer. Cell Stem Cell 6: 603–615.
20. Huang EH, Hynes MJ, Zhang T, Ginestier C, Dontu G, et al. (2009) Aldehyde dehydrogenase 1 is a marker for normal and malignant human colonic stem cells (SC) and tracks SC overpopulation during colon tumorigenesis. Cancer Res 69: 3382–3389.
21. Ding XW, Wu JH, Jiang CP (2010) ABCG2: a potential marker of stem cells and novel target in stem cell and cancer therapy. Life sciences 86: 631–637.
22. Schepers AG, Snippert HJ, Stange DE, van den Born M, van Es JH, et al. (2012) Lineage tracing reveals Lgr5+ stem cell activity in mouse intestinal adenomas. Science 337: 730–735.
23. Patrawala L, Calhoun T, Schneider-Broussard R, Zhou J, Claypool K, et al. (2005) Side population is enriched in tumorigenic, stem-like cancer cells, whereas ABCG2+ and ABCG2− cancer cells are similarly tumorigenic. Cancer Res 65: 6207–6219.
24. Challen GA, Little MH (2006) A side order of stem cells: the SP phenotype. Stem cells 24: 3–12.
25. Gao N, White P, Kaestner KH (2009) Establishment of intestinal identity and epithelial-mesenchymal signaling by Cdx2. Developmental cell 16: 588–599.
26. Chan CW, Wong NA, Liu Y, Bicknell D, Turley H, et al. (2009) Gastrointestinal differentiation marker Cytokeratin 20 is regulated by homeobox gene CDX1. Proceedings of the National Academy of Sciences of the United States of America 106: 1936–1941.
27. Tot T (2002) Cytokeratins 20 and 7 as biomarkers: usefulness in discriminating primary from metastatic adenocarcinoma. Eur J Cancer 38: 758–763.
28. Dennis JL, Hvidsten TR, Wit EC, Komorowski J, Bell AK, et al. (2005) Markers of adenocarcinoma characteristic of the site of origin: development of a diagnostic algorithm. Clinical cancer research : an official journal of the American Association for Cancer Research 11: 3766–3772.
29. Moll R, Lowe A, Laufer J, Franke WW (1992) Cytokeratin 20 in human carcinomas. A new histodiagnostic marker detected by monoclonal antibodies. The American journal of pathology 140: 427–447.
30. Bayrak R, Haltas H, Yenidunya S (2012) The value of CDX2 and cytokeratins 7 and 20 expression in differentiating colorectal adenocarcinomas from extraintestinal gastrointestinal adenocarcinomas: cytokeratin 7−/20+ phenotype is more specific than CDX2 antibody. Diagn pathol 7: 9.
31. Ee HC, Erler T, Bhathal PS, Young GP, James RJ (1995) Cdx-2 homeodomain protein expression in human and rat colorectal adenoma and carcinoma. The American journal of pathology 147: 586–592.
32. Stratton MR, Campbell PJ, Futreal PA (2009) The cancer genome. Nature 458: 719–724.
33. Dean M, Fojo T, Bates S (2005) Tumour stem cells and drug resistance. Nature reviews Cancer 5: 275–284.
34. Inoda S, Hirohashi Y, Torigoe T, Morita R, Takahashi A, et al. (2011) Cytotoxic T lymphocytes efficiently recognize human colon cancer stem-like cells. The American journal of pathology 178: 1805–1813.
35. Rosen JM, Jordan CT (2009) The increasing complexity of the cancer stem cell paradigm. Science 324: 1670–1673.
36. Werling RW, Yaziji H, Bacchi CE, Gown AM (2003) CDX2, a highly sensitive and specific marker of adenocarcinomas of intestinal origin: an immunohistochemical survey of 476 primary and metastatic carcinomas. The American journal of surgical pathology 27: 303–310.
37. Chiou SH, Yu CC, Huang CY, Lin SC, Liu CJ, et al. (2008) Positive correlations of Oct-4 and Nanog in oral cancer stem-like cells and high-grade oral squamous cell carcinoma. Clinical cancer research : an official journal of the American Association for Cancer Research 14: 4085–4095.
38. Schoenhals M, Kassambara A, Vos JD, Hose D, Moreaux J, et al. (2009) Embryonic stem cell markers expression in cancers. Biochem Biophys Res Commun 383: 157–162.
39. Saigusa S, Tanaka K, Toiyama Y, Yokoe T, Okugawa Y, et al. (2009) Correlation of CD133, OCT4, and SOX2 in Rectal Cancer and Their Association with Distant Recurrence After Chemoradiotherapy. Annals of Surgical Oncology 16: 3488–3498.
40. Neumann J, Bahr F, Horst D, Kriegl L, Engel J, et al. (2011) SOX2 expression correlates with lymph-node metastases and distant spread in right-sided colon cancer. BMC Cancer 11: 518.
41. Yu F, Li J, Chen H, Fu J, Ray S, et al. (2011) Kruppel-like factor 4 (KLF4) is required for maintenance of breast cancer stem cells and for cell migration and invasion. Oncogene 30: 2161–2172.
42. Matsuoka J, Yashiro M, Sakurai K, Kubo N, Tanaka H, et al. (2012) Role of the Stemness Factors Sox2, Oct3/4, and Nanog in Gastric Carcinoma. J Surg Res 174: 130–135.
43. Hong H, Takahashi K, Ichisaka T, Aoi T, Kanagawa O, et al. (2009) Suppression of induced pluripotent stem cell generation by the p53-p21 pathway. Nature 460: 1132–1135.

**Figure S1**

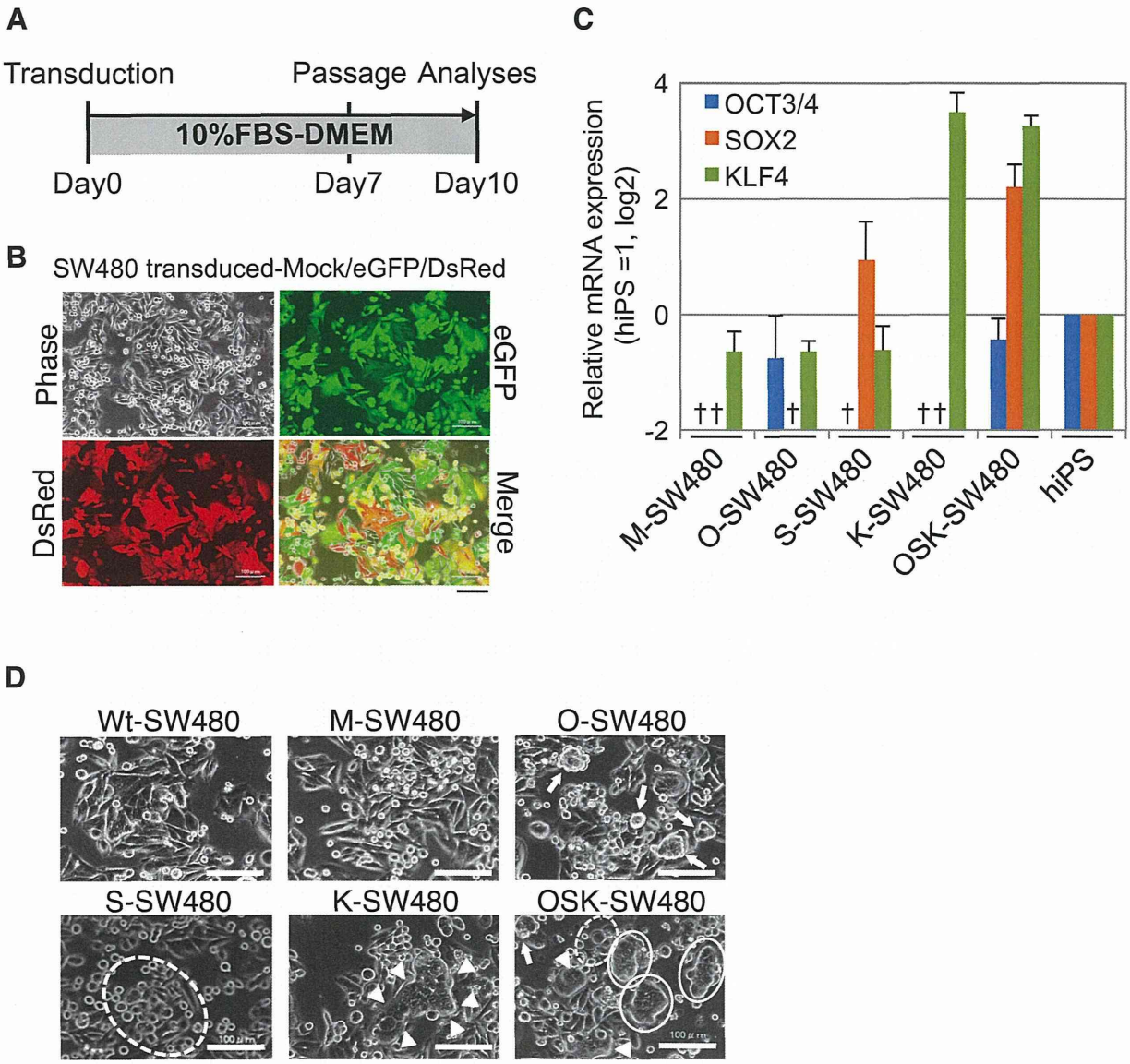
A
Transduction
Passage
Analyses
10%FBS-DMEM
Day0
Day7
Day10
B
SW480 transduced-Mock/eGFP/DsRed
Phase
eGFP
DsRed
Merge
C
Relative mRNA expression
(hiPS =1, log2)
4
2
0
-2
OCT3/4
SOX2
KLF4
††
†
†
††
M-SW480
O-SW480
S-SW480
K-SW480
OSK-SW480
hiPS
D
Wt-SW480
M-SW480
O-SW480
S-SW480
K-SW480
OSK-SW480
100 μm

**Figure S2**

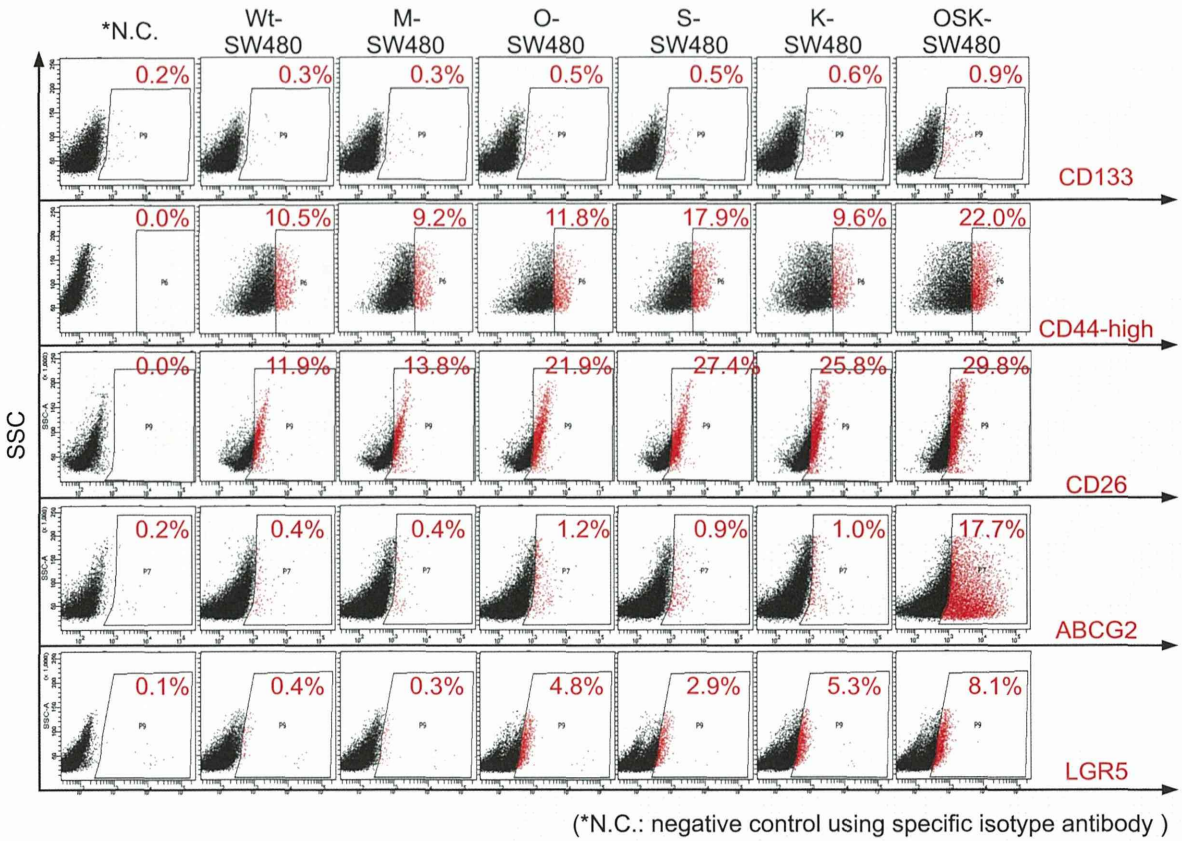


(*N.C.: negative control using specific isotype antibody )

**Figure S3**

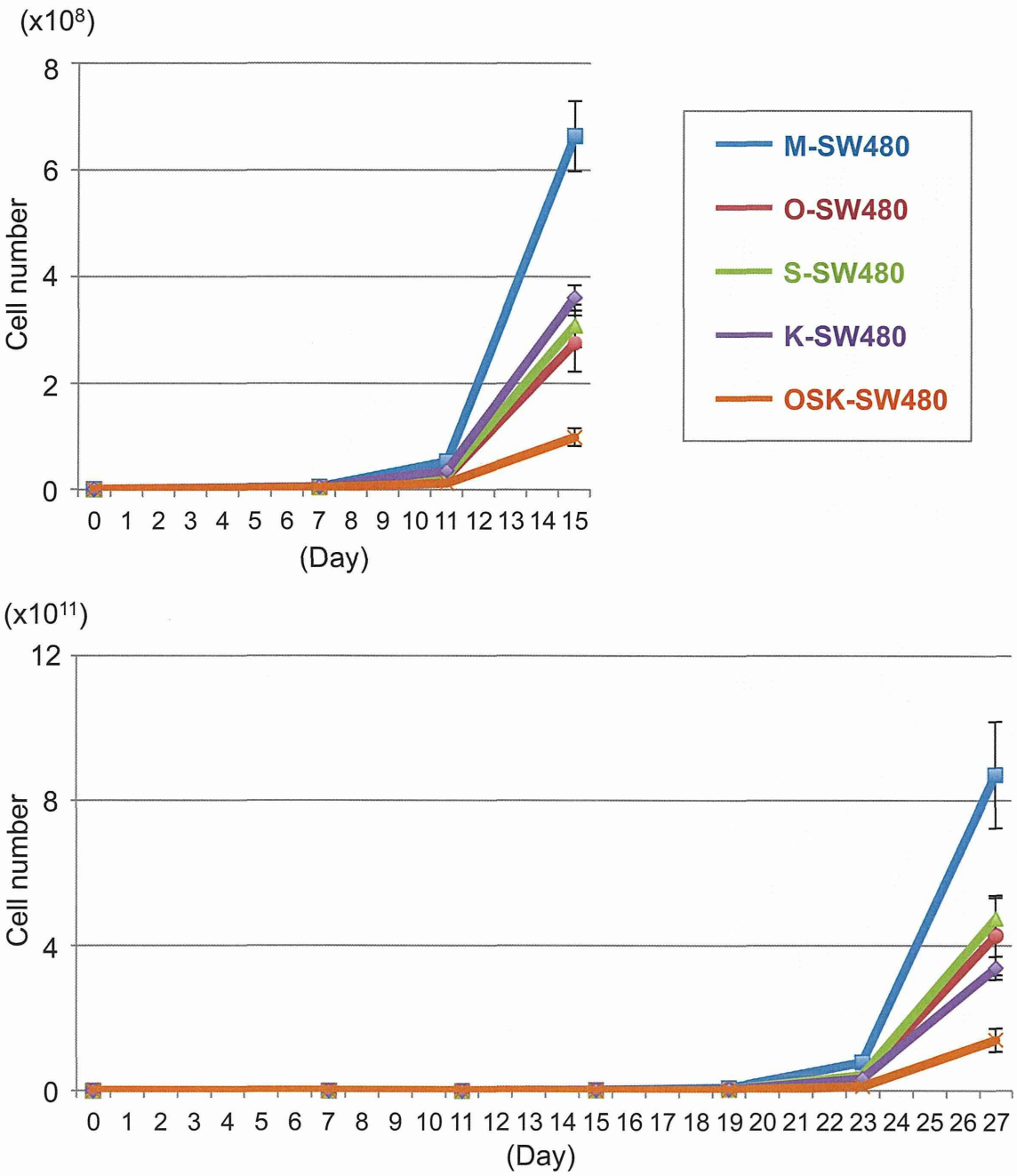
(x10^8)
Cell number
(Day)
M-SW480
O-SW480
S-SW480
K-SW480
OSK-SW480
(x10^11)
Cell number
(Day)

**Figure S4**

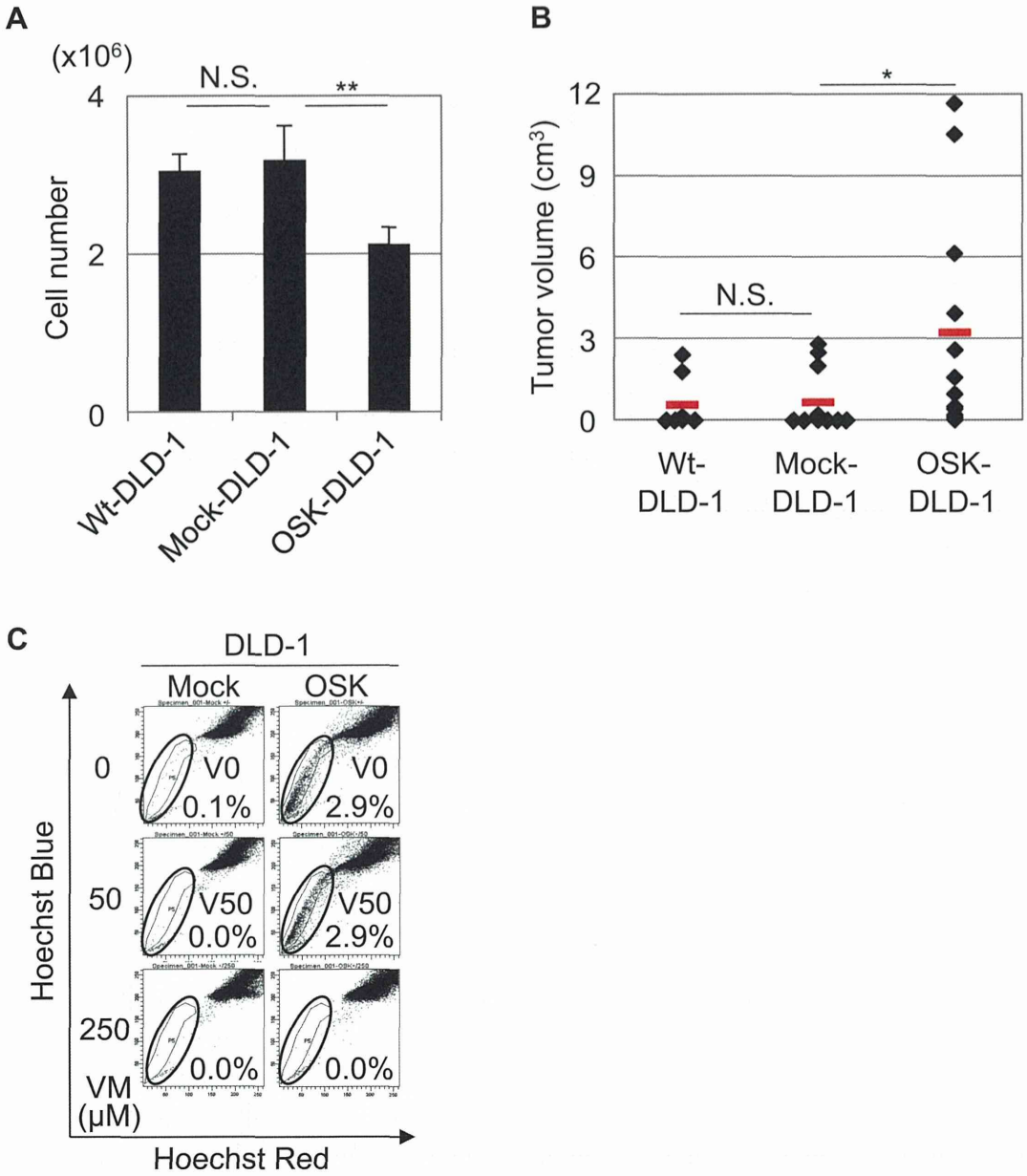
A
(x10⁶)
N.S.
**
Cell number
4
2
0
Wt-DLD-1
Mock-DLD-1
OSK-DLD-1
B
*
12
9
6
3
0
Tumor volume (cm³)
N.S.
Wt-DLD-1
Mock-DLD-1
OSK-DLD-1
C
DLD-1
Mock
OSK
0
50
250
VM (μM)
V0
0.1%
V0
2.9%
V50
0.0%
V50
2.9%
0.0%
0.0%
Hoechst Blue
Hoechst Red

**Figure S5**

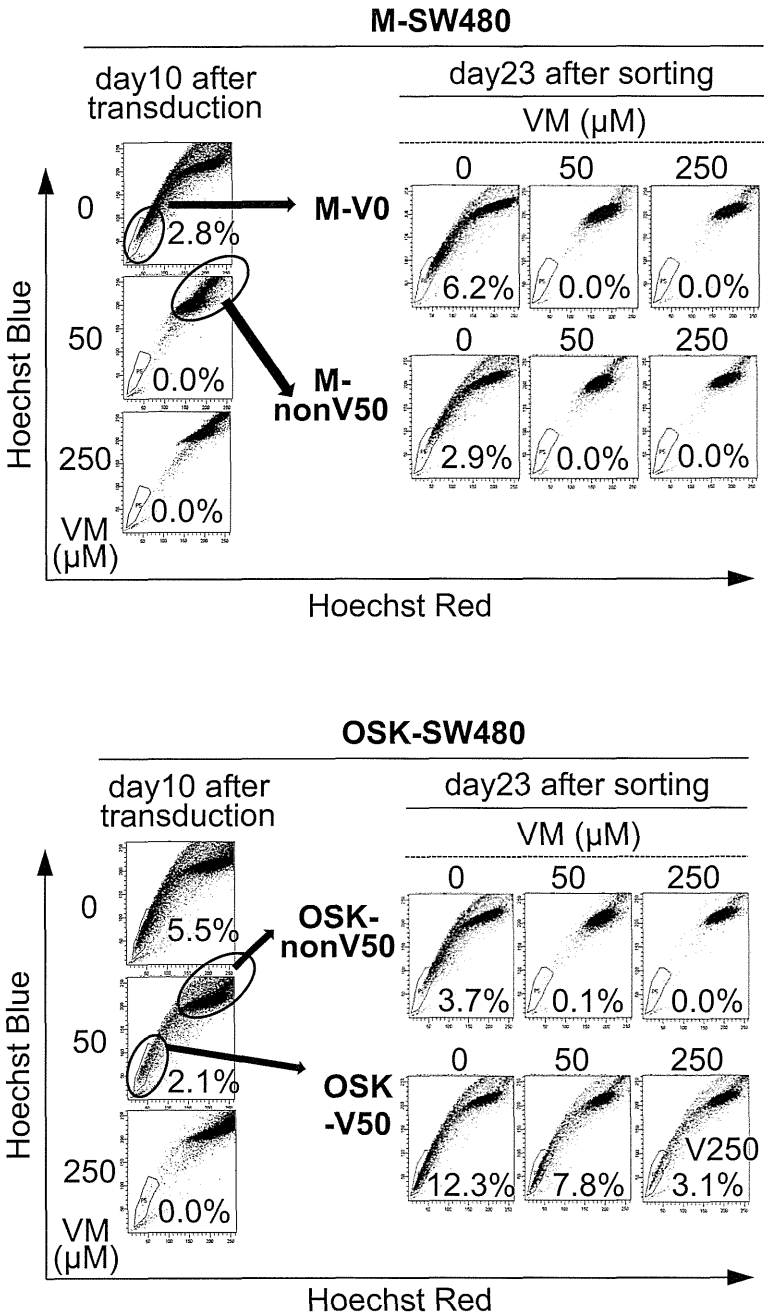
M-SW480
day10 after transduction
day23 after sorting
VM (μM)
0
50
250
2.8%
0.0%
0.0%
M-V0
M-nonV50
6.2%
0.0%
0.0%
2.9%
0.0%
0.0%
Hoechst Blue
Hoechst Red
OSK-SW480
5.5%
2.1%
0.0%
OSK-nonV50
OSK-V50
3.7%
0.1%
0.0%
12.3%
7.8%
V250
3.1%

**Figure S6**

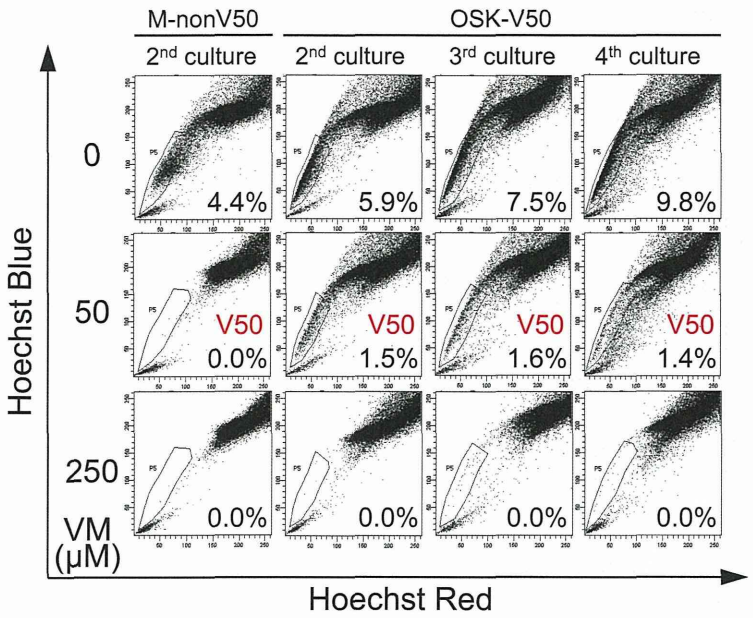
M-nonV50
OSK-V50
2nd culture
2nd culture
3rd culture
4th culture
0
50
250
VM (μM)
4.4%
5.9%
7.5%
9.8%
V50
0.0%
V50
1.5%
V50
1.6%
V50
1.4%
0.0%
0.0%
0.0%
0.0%
Hoechst Blue
Hoechst Red

**Figure S7**

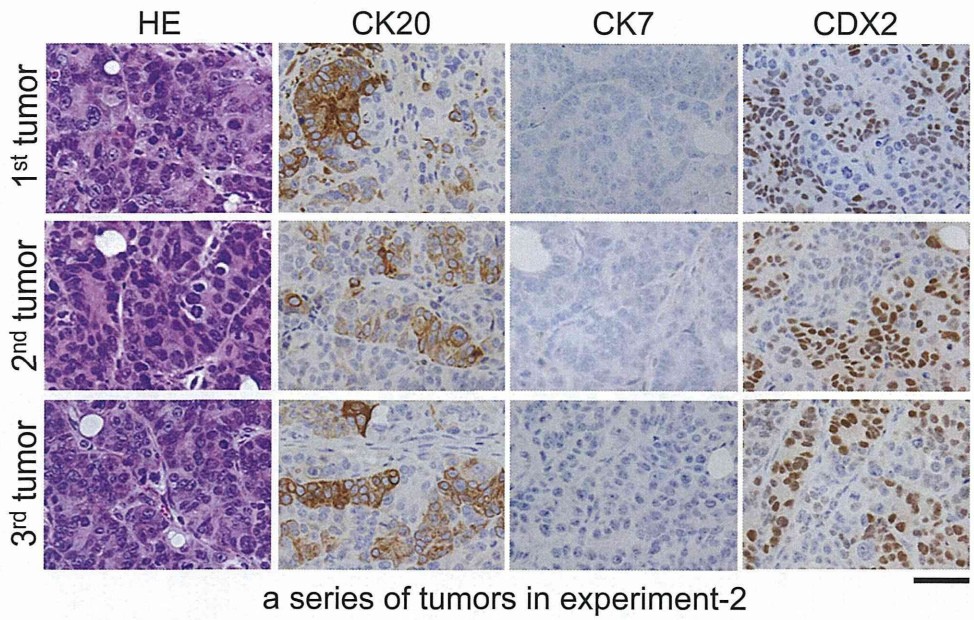


a series of tumors in experiment-2

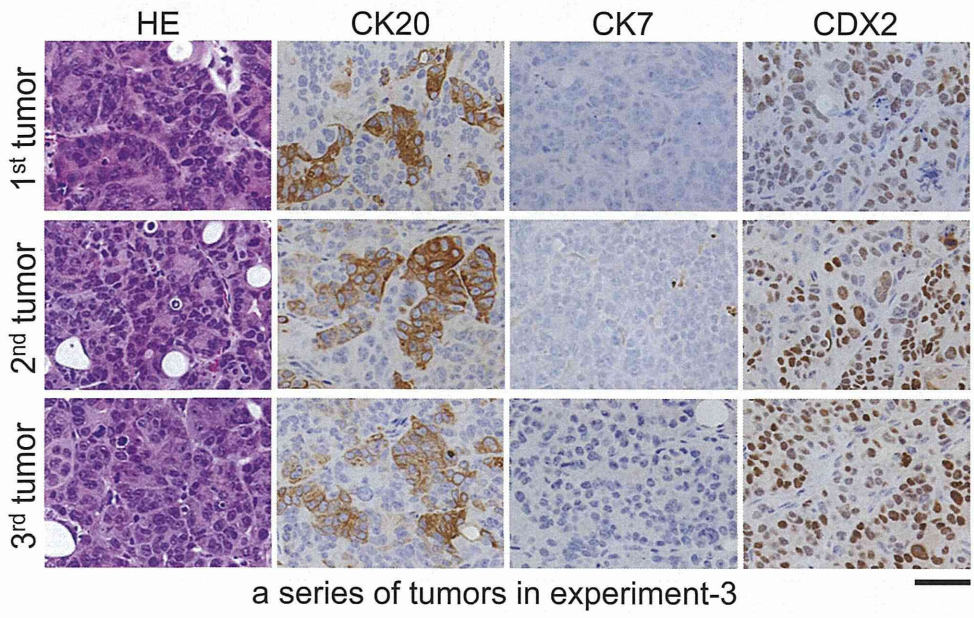


a series of tumors in experiment-3

## Figure S8

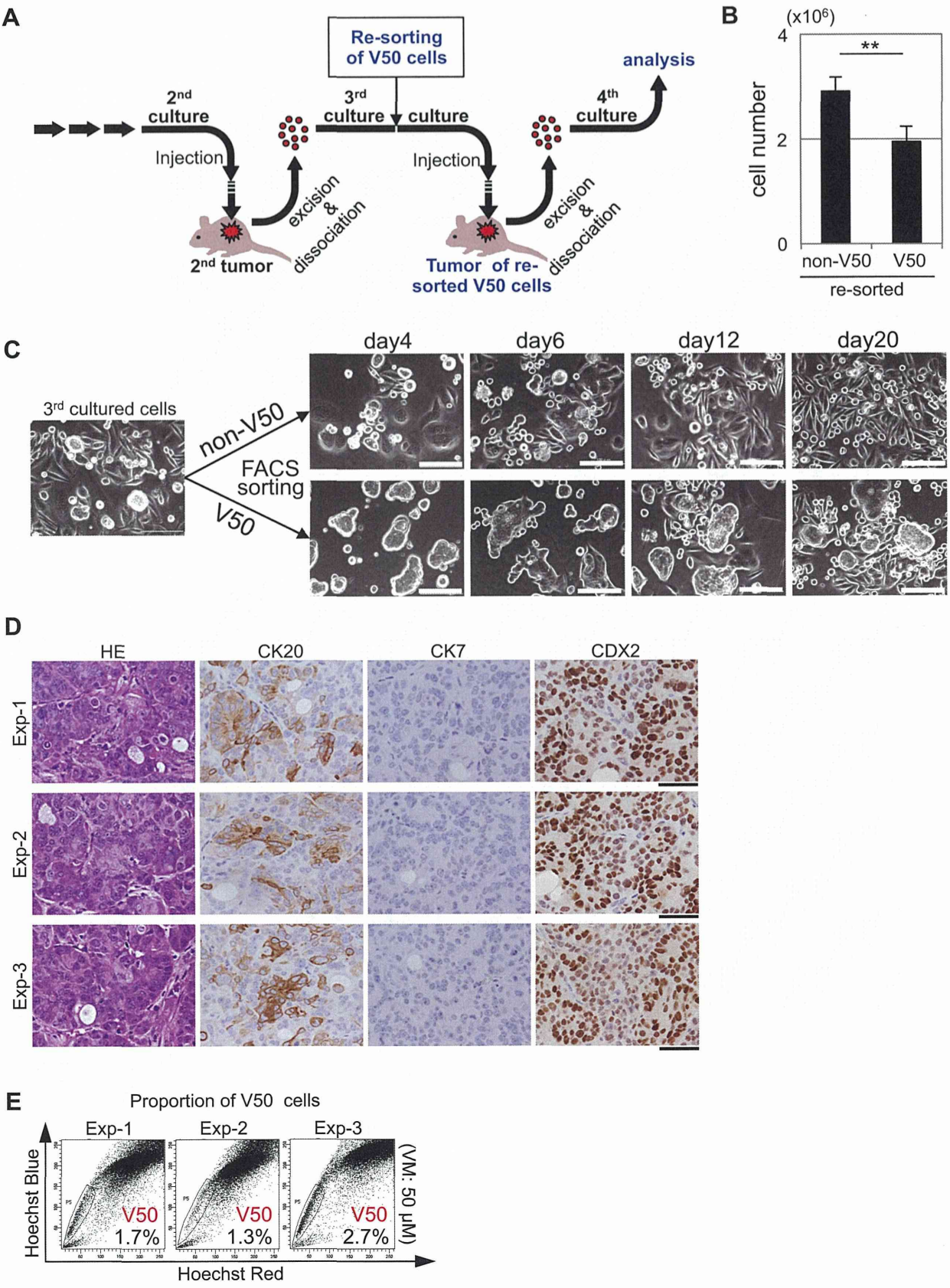
A
Re-sorting of V50 cells
2nd culture
3rd culture
4th culture
analysis
Injection
Injection
excision & dissociation
excision & dissociation
2nd tumor
Tumor of re-sorted V50 cells
B
(x10⁶)
cell number
**
non-V50
V50
re-sorted
C
day4
day6
day12
day20
3rd cultured cells
non-V50
FACS sorting
V50
D
HE
CK20
CK7
CDX2
Exp-1
Exp-2
Exp-3
E
Proportion of V50 cells
Exp-1
Exp-2
Exp-3
Hoechst Blue
Hoechst Red
V50 1.7%
V50 1.3%
V50 2.7%
(VM: 50 μM)

**Table S1**

Primer sequences used in qRT-PCR

| Target gene | Sequence (5' to 3') |
|---|---|
| hOCT3/4(endo and trans) | CCC CAG GGC CCC ATT TTG GTA CC |
| | ACC TCA GTT TGA ATG CAT GGG AGA GC |
| hSOX2(endo and trans) | TTC ACA TGT CCC AGC ACT ACC AGA |
| | TCA CAT GTG TGA GAG GGG CAG TGT GC |
| hKLF4(endo and trans) | CAT GCC AGA GGA GCC CAA GCC AAA GAG GGG |
| | CGC AGG TGT GCC TTG AGA TGG GAA CTC TTT |
| CD44 | AGA AGG TGT GGG CAG AAG AA |
| | AAA TGC ACC ATT TCC TGA GA |
| CD26 | CAA ATT GAA GCA GCC AGA CA |
| | CAC ACT TGA ACA CGC CAC TT |
| CD133 | TGG GGC TGC TGT TTA TTA TTC T |
| | TGC CAC AAA ACC ATA GAA GAT G |
| ALDH1 | TCC TGG TTA TGG GCC TAC AG |
| | CTG GCC CTG GTG GTA GAA TA |
| ABCG2 | AGC TGC AAG GAA AGA TCC AA |
| | TCC AGA CAC ACC ACG GAT AA |
| LGR5 | GAT GTT GCT CAG GGT GGA CT |
| | TTT CCC GCA AGA CGT AAC TC |
| GAPDH | ACC ACA GTC CAT GCC ATC AC |
| | TCC ACC ACC CTG TTG CTG TA |

**Table S2**

Summary of tumor formation derived from transduced DLD-1 cells

| | Tumor formation |
|---|---|
| | Injected cell number |
| Cell name | 1 x$10^5$ |
| Wt-DLD-1 | 50% (4/8) |
| Mock-DLD-1 | 50% (6/12) |
| OSK-DLD-1 | 91.6% (11/12) |

# 生体肝移植（小児例）

## —小児生体肝移植—

神戸国際フロンティアメディカルセンター　田中 紘一、山田 貴子

### 1．生体肝移植は小児で始まった

健常人をドナーとする生体肝移植は、海外でも日本でも小児生体肝移植で始まった。しかしながらその導入に至る経緯は極めて違った。欧米では、1980年代になり、肝疾患末期状態患者への救命治療として脳死肝移植が確立・普及した。その結果、移植希望者が増え相対的ドナー不足が次第に深刻となったが、特に小児移植で著しかった。この解決法として、成人ドナー肝を用いる部分肝移植や2人のレシピエントに移植する分割肝移植が発展してきた[1]。しかし、ドナープールの拡大には結びつかず、部分肝移植の手技を用いる生体肝移植が1989年にシカゴ大学で系統的に導入され、これを起点に同法は発展してきた。一方、わが国では脳死臓器移植が容認されなかったため、患者は渡航移植に活路を求め海外のドナープールへ影響を及ぼしてきた。アカデミア側は、脳死肝移植を目指し1980年に肝移植懇談会（後の肝移植研究会）を発足させ、臨床応用を目指して基礎的研究を行い、その成果で大きく世界に貢献してきた。一方、生体肝移植については1990年までに、いくつかの大学で、動物を用いる生体肝移植の実験が行われてきた。京都大学では、水本らがイヌを用いて70％の部分肝を、左側腎摘後異所性に移植する方法や同所性移植法を1974年に発表したが、免疫抑制剤がアザチオプリン時代であったこともあって臨床に結びつかなかった[2]。1980年代になると、肝臓外科研究、肝臓外科手術や小児外科手術の進歩、ブタを用いる全肝移植研究、肝サポート研究等が連鎖し、生体肝移植の臨床実現の気運となった。田中らは1987年から2年間に亘って、イヌの左側葉を、全肝摘出したイヌに移植する動物実験を繰り返した[3]。同じ頃、佐々木睦夫らは弘前大学で、河原崎秀雄らは浜松医科大学と東京大学で動物実験を実施していた。これら実験中に、1988年には世界の第一例をRiaらがブラジル・サンパウロで行い、翌年、オーストラリア・ブリスベーンでStrongらが実施し、世界で初めて成功した。わが国では、1989年11月に島根医科大学の永末らが、胆道閉鎖症の小児に緊急生体肝移植を実施して、臨床の口火を切った（図1）。1990年6月には京都大学で、次いで信州大学と続き、わが国の生体肝移植の幕開けとなった。

このようにわが国では、脳死臓器移植の実績なしで生体肝移植が展開されたが、これを発展させたのは、脳死臓器移植が容認されてない中で、あらゆる分野の方々の尽力によるものであった。Broelshらは1994年のHepatologyで、世界の生体肝移植（小児例）の150例を集積し、大


1989年、島根医大で国内初の生体肝移植
「家族の願い」道開く
揺れた祖母も決意
2つの命
いまや世界をリード
倫理委 2件承認、実施はゼロ

図 1. 1989 年島根医科大学で国内初の生体肝移植

部分が米国と日本で行われ、成績もよいと評価して紹介している[4]。しかしながら、親から子への生体肝移植導入の頃は、健常人の手術が必要であること、精神的・社会的ストレスをもたらすこと、倫理的側面等で大きな課題が論議された[5]。

## 2. 小児生体肝移植の世界への貢献

小児生体肝移植をわが国から世界に発信した主な点は、手術手技の開発、免疫抑制剤タクロリムスの臨床応用、免疫抑制剤の減量・離脱、HBc 抗体陽性ドナーからのＢ型肝炎ウイルス伝播、ABO 血液型不適合移植、海外への普及にある。

### 1）手術手技の開発（図 2）

手術手技で、世界の多くの論文にとりあげられるのは、ドナーの肝切除法と移植手技[6]、マイクロサージャリーによる肝動脈吻合[7]、新生児・乳児症例に対する単区域グラフト移植である[8]。

生体肝移植では、血管グラフト利用が制限されるので、動脈閉塞による移植肝不全を避けねばならない。さらに脳死ドナーのバックアップが不可能であり、再移植が極めて困難である。欧米では肝移植後、肝動脈閉鎖が小児で高いとの報告があり、この克服のため、世界で初めてマイクロサージャリーによる肝動脈再建を導入し、発生率が著しく低下した。これ以後、マイクロサージャリーによる肝動脈再建は、世界のスタンダードとなった[7]。サイズマッチは、小児では大きな問題とならないが、新生児・乳児症例では、肝外側葉が過大となり、レシピエントからの少な